https://dx.doi.org/10.1016/j.ymssp.2019.106568

This is the Pre-Published Version.

Analytical solution to temperature-induced deformation of suspension bridges

Yi ZHOU[1,2], Yong XIA[2], Bo CHEN[3], Yozo FUJINO[4]

[1] Beijing Key Laboratory of Urban Underground Space Engineering, University of Science & Technology Beijing, Beijing 100083, China

[2] Department of Civil and Environmental Engineering, The Hong Kong Polytechnic University, Hong Kong, China

[3] Key Laboratory of Roadway Bridge and Structural Engineering, Wuhan University of Technology, Wuhan 430070, China

[4] Institute of Advanced Sciences, Yokohama National University, Yokohama 240-8501, Japan

Correspondence: zhouyi@ustb.edu.cn (Y. ZHOU); cey-xia@polyu.edu.hk (Y. XIA)

Abstract

Varying ambient temperature may cause significant deformation of long-span suspension bridges. This study investigates the mechanisms of the temperature-induced mid-span deflection and tower-top horizontal displacement of suspension bridges, and formulates the general analytical solutions to the thermal responses of ground anchored suspension bridges. The temperature-induced mid-span deflection can be determined from the superposition of deflections caused by each of the separate temperature changes of the main-span cable, side-span cables, and towers, while the tower-top horizontal displacement is a combination of the thermal effects of the side-span cables and towers. It is found that the cable temperature plays the dominant role in the mid-span deflection and tower-top horizontal displacement. Moreover, the temperature effective length is proposed and a unified formula of the temperature-induced bridge responses is obtained. The accuracy of the proposed formulas is verified through the field monitoring data of the 2132-m-long Tsing Ma Bridge at Hong Kong. The present study not only provides a simple, general, and unified analytical solution to the temperature-induced deformation of long-span suspension bridges, but also assists engineers in understanding the mechanisms of thermal behaviours of such bridges.

Keywords

Suspension bridge; thermal deformation; mechanism; analytical model; structural health monitoring

Nomenclature

f_0	The mid-span deflection of the main-span cable of a suspension bridge. It is measured positive downward from the cable chord. The temperature-induced

© 2019. This manuscript version is made available under the CC-BY-NC-ND 4.0 license http://creativecommons.org/licenses/by-nc-nd/4.0/

	variation of f_0 is denoted as δf_0.
δD_0	The temperature-induced variation in the mid-span elevation of the main-span cable of a suspension bridge. It is positive when the mid-point of the cable goes upward.
n	The sag-to-span ratio of the main-span cable
l_i	The horizontal distance (or span) between the two end supports of the main-, left side-, and right side-span cables, which correspond to $i = 0, 1, 2$ respectively
h_i	The vertical distance (or elevation difference) between the two end supports of the main-, left side-, and right side-span cables with $i = 0, 1, 2$
h_{Pi}	The height of tower i, with $i = 1, 2$ being the left and right towers
α	The slope of the chord of the main-span cable, with a positive value for the counter clockwise rotation from the horizontal
δT_j	The temperature variation of the cable ($j = \mathrm{C}$) or the tower ($j = \mathrm{P}$)
θ_j	The linear expansion coefficient of the cable ($j = \mathrm{C}$) or the tower ($j = \mathrm{P}$)

1. Introduction

The cyclic variation in ambient temperature may cause considerable deformation of bridges, which may outweigh those induced by traffic or wind loading, especially for long-span suspension bridges[1]. The temperature related quasi-static responses need to be ascertained and then subtracted from the overall measurements, in order to detect the undesirable deformation due to structural anomalies and/or deterioration. The temperature effects of bridges have attracted intensive attention in the bridge community, e.g., the case studies on the arch bridges[2, 3], cable-stayed bridges[4, 5], and suspension bridges[6, 7].

Suspension bridges have the longest spanning ability but the least global stiffness, and are thus vulnerable to excessive deformation under operational and environmental actions. Moreover, on account of the complicated configuration with multiple inter-linked components, it is practically

difficult to predict the responses of a suspension bridge to real actions accurately using the ideal numerical model based on the design. Early structural health monitoring (SHM) systems developed in the last century were mainly installed on suspension bridges to monitor their on-site behaviours. For example, Xu et al.[6] utilized the long-term monitoring data of the Tsing Ma Bridge in Hong Kong to investigate the statistical relationship between the effective girder temperature and the structural displacements. Xia et al.[8] further investigated the temperature distribution and thermal responses of the bridge through heat transfer analysis and structural analysis, respectively. Koo et al.[9] presented the field measurements of Tamar Bridge, a suspension bridge with a 335 m main span, and found that the temperature change was the most influential driver of the structural deformation compared with the other actions. Later, Westgate et al.[10] reproduced the temperature distribution and structural quasi-static responses of this bridge using the finite element (FE) analysis. Kashima et al.[11] reported that the girder of the Akaishi Kaikyo Bridge lowered about 2 m at the mid-span when the cable temperature increased from 0 to 30 ºC, and this elevation change had a higher linear correlation with the cable temperature than the atmospheric temperature.

Other case studies on the thermal deformation of suspension bridges include Runyang Suspension Bridge (with a main span of 1490 m)[12], Humber Bridge (1410 m)[7], Jiangyin Bridge (1385 m)[13], Yangluo Bridge (1280 m)[14], Yeongjong Bridge (300 m)[15], Hunan Road Bridge (112 m)[16]. When temperature increases, the girders of these bridges undergo significant axial extension, and their central spans consistently curve downward, similar as the Tsing Ma, Tamar, and Akaishi Kaikyo bridges.

The previous studies showed that the longitudinal displacement of the bridge girders is determined by the thermal expansion or contraction, which can be estimated with a good accuracy from the formula $\delta L_{\text{org}} = \theta \cdot L_{\text{org}} \cdot \delta T$, where $\delta(\cdot)$ represents the change of a quantity and L_{org}, T, and θ respectively denote the original free length, temperature, and linear expansion coefficient of the girder. Regarding to other thermal deformation of suspension bridges, e.g. the mid-span deflection and tower sway, there is no simple general formula. These responses are usually predicted via the regression or FE analyses, both being case by case and lacking generality. Moreover, the regression

analysis relies on a lot of measurement data and masks the mechanisms behind the model, while the FE analysis is generally time consuming and non-intuitive as to interpretation of the results.

Although some simplified analytical models of suspension bridges are available in the structural preliminary design, they deal with the deformation caused by traffic or wind loads[17]. For temperature loading, only simplified consideration has been given to the mid-span deflection due to the temperature change in the main-span cable; there is neither analytical solution to tower-top displacement nor consideration of the temperature change in the side-span cables and towers[18].

This study aims: (1) to reveal the underlying mechanisms of the temperature-induced mid-span deflection and tower-top horizontal displacement of suspension bridges; and (2) to propose physics-based and general formulas of temperature-induced displacements which can be applied to suspension bridges having different geometric dimensions. The proposed analytical model and the formulas are verified by using the field monitoring data of the Tsing Ma Bridge.

2. Formulae Development

Consider a two-tower ground anchored suspension bridge as shown in Figure 1. In the formula development, we assume that: (1) The sag of the side-span cables is negligible; (2) The cable is inelastic without elastic deformation; (3) The flexurale stiffness of the tower and girder is omitted. f_0 is the vertical distance between the cable chord and the cable at the mid-span. Throughout this paper, f_0 is also called the sag and is positive downward relative to the cable chord. Without losing the generality, the bridge model has two towers with a height of h_{Pi} ($i=1,2$), whose tops are not necessarily at the same level. The suspension cable is divided by the towers into three spans with the horizontal distances of l_1, l_0, and l_2, respectively. The vertical distances between the two end supports of the left side-, main-, and right side-span cables are h_1, h_0, and h_2. If the inclination angle of the chord of the main-span cable is α, then l_0 and h_0 can be related as $h_0 = l_0 \tan\alpha$. The total horizontal distance between the two anchor blocks is $L = \sum_{i=0}^{2} l_i$. Special attention should be paid to the connection and boundary conditions. While always firmly secured at the anchorages, the main

Commented [XY1]: What does this mean? Do you mean that: the flexural deformation of the tower and girder is neglected?

cables are also fixed at the tower tops without relative sliding during the operational stage. The girder can move freely along the bridge axis at both girder–tower intersections.

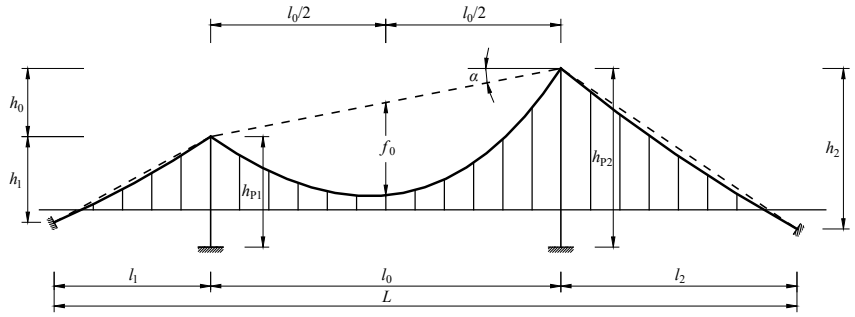

Figure 1 Schematic configuration of a general two-tower ground anchored suspension bridge

For a ground anchored suspension bridge, the expansion or contraction of the girder induced by the change in average girder temperature has little influence on the vertical displacement of the cable. Meanwhile, the girder is analogue to an elastically supported continuous beam owing to the ~~hangers~~suspenders. The elevation of the mid-span is almost unaffected by the temperature difference between the top and bottom surfaces of the girder, as reported in Ref. [19]. Therefore, the vertical differential temperature of the girder contributes little to the sag change of the main-span cable. As a result, the variation of f_0 can be approximated as a combination of thermal effects of the following three components: (1) the main-span cable; (2) the side-span cables; and (3) the towers. The three effects are investigated in the following sections.

2.1 Factor 1: Effects of temperature change in the main-span cable

The mid-span deflection variation of the main-span cable due to its own temperature increase can be estimated based on the analytical model of a single cable suspended at both ends shown in Figure 2. The length of the cable, S_0, is approximated as:

$$S_0 = l_0\left[\sec\alpha + \frac{8}{3}n^2\cos^3\alpha - \frac{32}{5}n^4\left(5\cos^7\alpha - 4\cos^5\alpha\right)\right] \quad (1)$$

where $n = f_0/l_0$ is the sag-to-span ratio of the cable. The mathematical derivation of Eqn. (1) is presented in Appendix A.

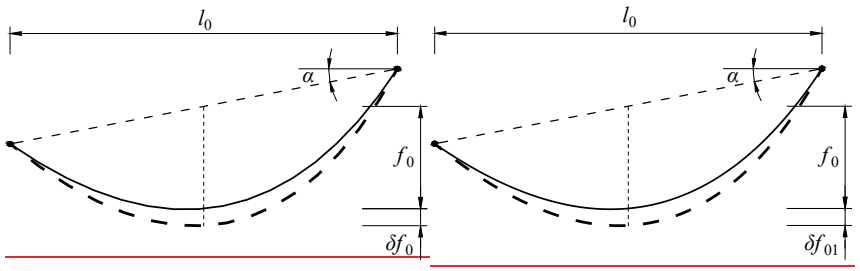

Figure 2 Mid-span deflection variation due to temperature change of the cable

The first variation of Eqn. (1) yields:

$$\delta S_0 = c_n \cdot \delta n + c_{l_0} \cdot \delta l_0 + c_\alpha \cdot \delta\alpha \tag{2}$$

The coefficients of δn, δl_0, and $\delta\alpha$ are:

$$c_n = l_0\left[\frac{16}{3}n\cos^3\alpha - \frac{128}{5}n^3\left(5\cos^7\alpha - 4\cos^5\alpha\right)\right] \tag{3}$$

$$c_{l_0} = \sec\alpha + \frac{8}{3}n^2\cos^3\alpha - \frac{32}{5}n^4\left(5\cos^7\alpha - 4\cos^5\alpha\right) \tag{4}$$

$$c_\alpha = l_0\left[\frac{\sin\alpha}{\cos^2\alpha} - 2n^2\left(\sin 3\alpha + \sin\alpha\right) + 32n^4\cos^4\alpha\sin\alpha\left(7\cos^2\alpha - 4\right)\right] \tag{5}$$

Utilizing $\delta l_0 = 0$, $\delta\alpha = 0$, and $\delta n = \delta f_0/l_0$, we have~~the first variation of Eqn. (1) yields~~:

$$\delta f_0 = \left[\frac{16}{3}n\cos^3\alpha - \frac{128}{5}n^3\left(5\cos^7\alpha - 4\cos^5\alpha\right)\right]^{-1} \cdot \delta S_0 \tag{26}$$

where δf_0 is the sag variation and the thermal elongation of the cable is $\delta S_0 = S_0 \cdot \theta_C \cdot \delta T_C$, with θ_C being the linear expansion coefficient of the material, and δT_C the temperature change in the cable.

According to the design specification for highway suspension bridges in China[20], the sag-to-span ratio n for main-span cables is usually between 1/11 and 1/9. Therefore, the higher-order terms

Field Code Changed

of n in Eqns. (1) and (62) can be omitted. The sag variation of the main-span cable due to its temperature change, δf_{01}, can be simplified as:

$$\delta f_{01} = \frac{3}{16n\cos^4\alpha} l_0 \theta_C \cdot \delta T_C \quad (73)$$

In Figure 2, the elongation of the main-span cable will reduce its tension force, which may result in a movement of the cable supports or the tower tops of the bridge. An FE analysis of the Tsing Ma Bridge shows that the tower-top displacements due to the temperature change in the main-span cable are negligible, as demonstrated in Appendix B. Therefore, both cable supports are assumed to remain unmoved in the above derivation. Also, ~~this study assumes~~ the effective temperature variation in the main cable is considered in this study while ~~have the same temperature variation along the length, and~~ the differential temperature ~~difference~~ on the cross section of the cable is ~~not considered~~neglected. This is because the former controls the longitudinal deformation of the cable while the latter has local effects only. ~~, as it does not change the cable length but causes local effects.~~

2.2 Factor 2: Effects of temperature change in the side-span cable

The thermal deformation of the side-span cable would cause the horizontal displacement of the tower top (Figure 3), and thus lead to the movement of the main-span cable. This effect will be analysed in following two steps. The first step establishes the relationship between the temperature changes in the side-span cables and the tower-top horizontal displacement, and the second determines the relation between the variation in the tower-top horizontal distance δl_0 and the mid-span deflection δf_0. Taking the left side-span cable as an example, Figure 3 illustrates the model of the first step analysis.

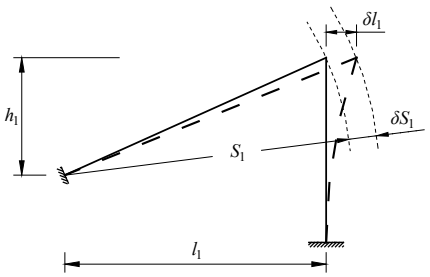

Figure 3 Tower-top horizontal displacement due to thermal expansion of the left side-span cable

Here, the side-span cable is assumed as straight and the small sag is negligible. Therefore, the chord length is used to approximate the cable length, i.e.,

$$S_1 = \sqrt{l_1^2 + h_1^2} \tag{84}$$

Taking the variation of Eqn. (48) and substituting $\delta S_1 = S_1 \cdot \theta_C \cdot \delta T_C$, we have:

$$\delta l_1 = \frac{l_1^2 + h_1^2}{l_1} \theta_C \cdot \delta T_C \tag{95}$$

In the second step analysis, the variation in the tower-top distance is based on the movement of both towers, i.e., $\delta l_0 = -(\delta l_1 + \delta l_2)$, as shown in Figure 4.

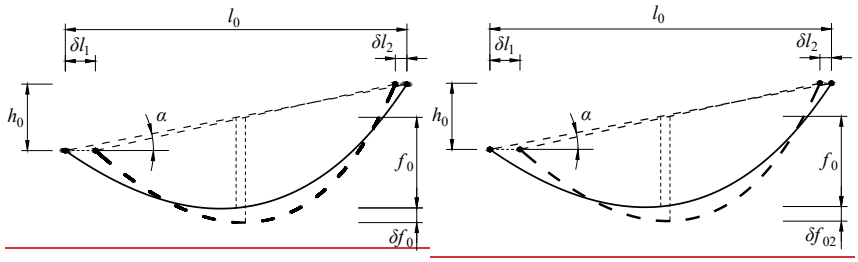

Figure 4 Mid-span deflection variation due to the tower-top horizontal movement

Take the first variations in S_0, n, l_0, and α still satisfy of Eqn. (21), and again. As in this case n, l_0, and α, and n vary, we have:

$$\delta S_0 = c_n \cdot \delta n + c_{l_0} \cdot \delta l_0 + c_\alpha \cdot \delta\alpha \quad (6)$$

Field Code Changed

Field Code Changed

~~The coefficients of δn, δl_0, and $\delta\alpha$ are:~~

~~$$c_n = l_0\left[\frac{16}{3}n\cos^3\alpha - \frac{128}{5}n^3\left(5\cos^7\alpha - 4\cos^5\alpha\right)\right] \quad (7)$$~~

~~$$c_{l_0} = \sec\alpha + \frac{8}{3}n^2\cos^3\alpha - \frac{32}{5}n^4\left(5\cos^7\alpha - 4\cos^5\alpha\right) \quad (8)$$~~

~~$$c_\alpha = l_0\left[\frac{\sin\alpha}{\cos^2\alpha} - 2n^2\left(\sin 3\alpha + \sin\alpha\right) + 32n^4\cos^4\alpha\sin\alpha\left(7\cos^2\alpha - 4\right)\right] \quad (9)$$~~

. The relationship between δn and δl_0 is:

$$\delta n = \delta\left(\frac{f_0}{l_0}\right) = \frac{l_0\cdot\delta f_0 - f_0\cdot\delta l_0}{l_0^2} \tag{10}$$

The elevation difference between the two tower tops, h_0, is invariant. Taking the variation of the equation $h_0 = l_0\tan\alpha$ and setting $\delta h_0 = 0$, we get the relationship between $\delta\alpha$ and δl_0:

$$\delta\alpha = -\frac{\sin 2\alpha}{2l_0}\delta l_0 \tag{11}$$

Substituting Eqns. (10) and (11) into Eqn. (~~6~~2) and setting $\delta S_0 = 0$, the relationship between δf_0 and δl_0 is obtained:

~~$$\delta f_0 = \left(n\frac{c_{l_0}}{c_n}l_0 + \frac{c_\alpha}{c_n}\sin 2\alpha\right)\delta l_0$$~~ $$\delta f_0 = \left(n - \frac{c_{l_0}}{c_n}l_0 + \frac{c_\alpha}{c_n}\cdot\frac{\sin 2\alpha}{2}\right)\cdot\delta l_0 \tag{12}$$

Expanding Eqn. (12) and omitting the higher-order terms of n will lead to:

~~$$\delta f_0 = \frac{3\cos 2\alpha}{16n\cos^4\alpha}\delta l_0$$~~ $$\delta f_0 = -\frac{3}{16n\cos^2\alpha}\cdot\delta l_0 \tag{13}$$

Eqn. (13) expresses the mid-span deflection variation of the main-span cable as an explicit function of δl_0, which depends on the movement of both tower tops. Combining Eqns. (~~5~~9) and (13), we will obtain the sag variation of the main-span cable induced by the temperature change in the side-span cables:

~~$$\delta f_{02} = \frac{3\cos 2\alpha}{16n\cos^4\alpha}\sum_{m=1}^{2}\left(\frac{l_m^2 + h_m^2}{l_m}\theta_C\cdot\delta T_C\right)$$~~ $$\delta f_{02} = \frac{3}{16n\cos^2\alpha}\sum_{m=1}^{2}\left(\frac{l_m^2 + h_m^2}{l_m}\theta_C\cdot\delta T_C\right) \tag{14}$$

In Figure 3, the variation in the cable tension due to the elongation of the cable is not taken into consideration. Appendix B demonstrates that the tension variation has a negligible effect on the tower-

top displacement of a real bridge.

2.3 Factor 3: Effects of temperature change in the tower

The thermal expansion or contraction of the towers will change the elevation of the tower top, which is also the end support of the side-span cable. Since the lower end of the cable is fixed at the anchorage and the length of the side-span cable does not change, the tower top will move ~~vertically and~~ horizontally (δl_1) and vertically (δh_{P1}), as illustrated in Figure 5. ~~Both~~The tower top movements ~~can~~ change the sag of the main-span cable, ~~and this effect~~which is also analysed in two steps. In the~~The~~ first step, ~~determines~~ the horizontal displacement δl_1 is determined.~~,~~ ~~and~~In the second step, ~~calculates~~ the mid-span deflection variation δf_0 due to δl_1 and δh_{P1} is calculated.~~The vertical movement δh_{P1} raises the main span cable but has little effect on the sag δf_0. The horizontal movement δl_1 changes the sag of the main span cable in a similar manner as Eqn. (13).~~

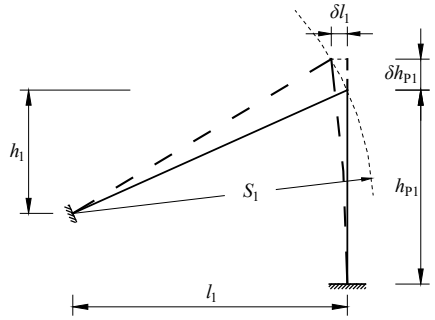

Figure 5 Tower-top ~~horizontallongitudinal~~ movement due to thermal expansion of the tower

In the first step ~~analysis~~, ~~T~~taking the variation of Eqn. (4~~8~~) with both l_1 and h_1 being variables, we have:

$$\delta S_1 = \frac{l_1}{\sqrt{l_1^2 + h_1^2}} \cdot \delta l_1 + \frac{h_1}{\sqrt{l_1^2 + h_1^2}} \cdot \delta h_1 \tag{15}$$

The length of the side-span cable is invariant, so $\delta S_1 = 0$. The elevation change of the tower top is

$$\delta h_1 = \delta h_{P1} = h_{P1} \theta_P \cdot \delta T_P \tag{16}$$

Field Code Changed

Field Code Changed

Commented [XY2]: Grammar error. First step CANNOT determine. 2ND step CANNOT calculate.

Field Code Changed

Commented [XY3]: I am confused here. Not clear and very confusing. Need to talk to you face to face or by phone. 2nd step is related to sag, however, first step is not.

Field Code Changed

Field Code Changed

Field Code Changed

Commented [XY4]: Here has both vertical and horizontal displacement

where θ_P is the linear expansion coefficient of the tower material; δT_P is the tower temperature variation; and δh_{P1} is the variation in the tower-top elevation. Based on Eqns. (15) and (16), we have:

$$\delta l_1 = -\frac{h_1}{l_1} \cdot \delta h_1 = -\frac{h_1}{l_1} h_{P1} \theta_P \cdot \delta T_P \tag{17}$$

As a result, the variation of the horizontal distance between both towers is

$$\delta l_0 = -(\delta l_1 + \delta l_2) = \sum_{m=1}^{2} \left(\frac{h_m \cdot h_{Pm}}{l_m} \cdot \theta_P \cdot \delta T_P \right) \tag{18}$$

In the second step ~~analysis~~, the tower top horizontal and vertical movement~~both the tower top horizontal distance variation and the tower top elevation variation~~ are taken into account, as shown in Figure 6.

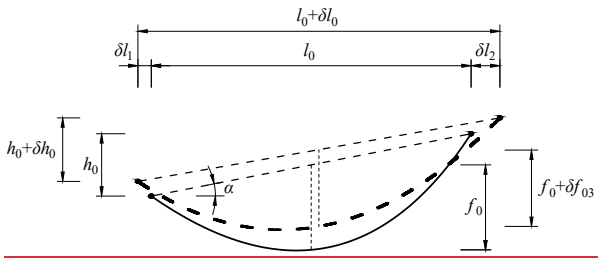

Figure 6 Mid-span deflection variation due to the tower-top horizontal and vertical movements

We take the first variation of the equation $h_0 = l_0 \tan\alpha$ again and ~~get~~have ~~$\delta\alpha =$~~:

$$\delta\alpha = \frac{\delta h_0 - \tan\alpha \cdot \delta l_0}{l_0 \cdot \sec^2 \alpha} \tag{19}$$

where $\delta h_0 = (h_{P2} - h_{P1}) \cdot \theta_P \cdot \delta T_P$. By ~~S~~substitutin~~g~~e Eqns. (3)–(5), (10), (18), and (19) into Eqn. (2) with the omission of the higher-order terms of n, and ~~by~~ setting $\delta S_0 = 0$, the mid-span deflection variation of the main-span cable as a result of the tower temperature change can be obtained:~~Given $\delta l_0 = -(\delta l_1 + \delta l_2)$ and Eqn. (13), the mid-span deflection variation of the main-span cable as a result of the tower temperature change is:~~

Field Code Changed

Commented [XY5]: This = "the tower top horizontal and vertical movement"

Field Code Changed

Field Code Changed

Field Code Changed

Field Code Changed

Field Code Changed

Field Code Changed

~~$$\delta f_{03} = \frac{3\cos 2\alpha}{16n\cos^4\alpha}\sum_{m=1}^{2}\left(\frac{h_m h_{\mathrm{P}m}}{l_m}\theta_{\mathrm{P}}\cdot\delta T_{\mathrm{P}}\right) \quad (18)$$~~

$$\delta f_{03} = -\frac{3}{16n\cdot\cos^2\alpha}\cdot\sum_{m=1}^{2}\left(\frac{h_m\cdot h_{\mathrm{P}m}}{l_m}\cdot\theta_{\mathrm{P}}\cdot\delta T_{\mathrm{P}}\right) - \frac{3\tan\alpha}{16n\cdot\cos^2\alpha}\left(h_{\mathrm{P}2}-h_{\mathrm{P}1}\right)\cdot\theta_{\mathrm{P}}\cdot\delta T_{\mathrm{P}} \quad (20)$$

~~It should be noted that~~ T~~t~~he first and second terms on the right side of Eqn. (20) respectively represent the influence of the horizontal and vertical movements of the tower tops on the mid-span sag change. ~~elevation change of the tower top, δh_{P1}, may affect t~~The inclination angle α takes positive values if ~~of~~ the chord of the main-span cable rotates counter clockwise from the horizontal~~, and this could change the sag of the main-span cable according to Eqn. (6)~~. Also, the tensions of the main- and side-span cables will change with δh_{P1}, which may induce additional movements of the tower top in Figure 5. Appendix B shows this ~~these two~~ effect~~s~~ is~~are~~ negligible and can thus be ignored herein.

Besides the average tower temperature, the differential temperature of the tower surfaces may also cause the horizontal displacement of the tower top[21], which is not considered in the present study for the following reasons: (1) Bridge towers are usually made of concrete, which has a low thermal conductivity. Therefore, only the tower surfaces have temperature difference and the tower inside has uniform temperature distribution[8]. Consequently, the differential temperature is not significant for concrete towers. (2) The tower-top span-wise displacement is constrained by both the main- and side-span cables, and the cable length is insensitive to the tower differential temperature. As a result, the position of the tower top has little change along the bridge axis direction.

2.4 Formulation of the total effects

The temperature-induced total variation in the mid-span deflection of the main-span cable is the algebraic sum of δf_{01}, δf_{02}, and δf_{03}:

~~$$\delta f_0 = \frac{3}{16n\cos^4\alpha}l_0\theta_{\mathrm{C}}\cdot\delta T_{\mathrm{C}} + \frac{3\cos 2\alpha}{16n\cos^4\alpha}\sum_{m=1}^{2}\left(\frac{l_m^2+h_m^2}{l_m}\theta_{\mathrm{C}}\cdot\delta T_{\mathrm{C}}\ \frac{h_m h_{\mathrm{P}m}}{l_m}\theta_{\mathrm{P}}\cdot\delta T_{\mathrm{P}}\right)$$~~

$$\delta f_0 = \frac{3}{16n\cdot\cos^4\alpha}\cdot l_0\cdot\theta_{\mathrm{C}}\cdot\delta T_{\mathrm{C}} + \frac{3}{16n\cdot\cos^2\alpha}\left[\sum_{m=1}^{2}\left(\frac{l_m^2+h_m^2}{l_m}\cdot\theta_{\mathrm{C}}\cdot\delta T_{\mathrm{C}} - \frac{h_m\cdot h_{\mathrm{P}m}}{l_m}\cdot\theta_{\mathrm{P}}\cdot\delta T_{\mathrm{P}}\right) - \left(h_{\mathrm{P}2}-h_{\mathrm{P}1}\right)\tan\alpha\cdot\theta_{\mathrm{P}}\cdot\delta T_{\mathrm{P}}\right]$$

(~~19~~21)

For most suspension bridges in practice, the two towers have equal elevation at the top, i.e., $\alpha = 0$. Hence, Eqn. (~~19~~21) can be simplified as:

$$\delta f_0 = \frac{3}{16n}\theta_{\mathrm{C}} l_0 \cdot \delta T_{\mathrm{C}} + \frac{3}{16n}\sum_{m=1}^{2}\left(\frac{l_m^2 + h_m^2}{l_m}\theta_{\mathrm{C}} \cdot \delta T_{\mathrm{C}} - \frac{h_m h_{\mathrm{P}m}}{l_m}\theta_{\mathrm{P}} \cdot \delta T_{\mathrm{P}}\right) \tag{~~20~~22}$$

For the majority of ground-anchored suspension bridges, $h_{\mathrm{P}m} \approx h_m$ ($m = 1, 2$). In the situation of rough estimation or without the tower temperature measurements, Eqn. (~~20~~22) can be further simplified with the assumptions of $h_{\mathrm{P}m} = h_m$ and $\theta_{\mathrm{C}} \cdot \delta T_{\mathrm{C}} = \theta_{\mathrm{P}} \cdot \delta T_{\mathrm{P}}$:

$$\delta f_0 = \frac{3}{16n} L\theta_{\mathrm{C}} \cdot \delta T_{\mathrm{C}} \tag{~~21~~23}$$

Note that the mid-span deflection of a cable is a relative quantity measured from the cable chord. It is different from the elevation change at the mid-span of the main-span cable, δD_0, which should include the variation of the tower height. The tower-top elevation change will change the position of the chord of the main-span cable at the mid-span, which is denoted as d_0:

$$d_0 = \frac{\delta h_{\mathrm{P1}} + \delta h_{\mathrm{P2}}}{2} = \frac{h_{\mathrm{P1}} + h_{\mathrm{P2}}}{2}\theta_{\mathrm{P}} \cdot \delta T_{\mathrm{P}} \tag{2~~4~~2}$$

Given the different sign definition of δf_0 and δD_0, the latter is calculated as $\delta D_0 = -\delta f_0 + d_0$, namely,

$$\delta D_0 = \frac{3}{16n\cos^4\alpha} l_0\theta_{\mathrm{C}} \cdot \delta T_{\mathrm{C}} \frac{3\cos 2\alpha}{16n\cos^4\alpha}\sum_{m=1}^{2}\left(\frac{l_m^2 + h_m^2}{l_m}\theta_{\mathrm{C}} \cdot \delta T_{\mathrm{C}} \frac{h_m h_{\mathrm{P}m}}{l_m}\theta_{\mathrm{P}} \cdot \delta T_{\mathrm{P}}\right) + \frac{h_{\mathrm{P1}} + h_{\mathrm{P2}}}{2}\theta_{\mathrm{P}} \cdot \delta T_{\mathrm{P}}$$

$$\delta D_0 = -\frac{3 \cdot l_0 \cdot \theta_{\mathrm{C}} \cdot \delta T_{\mathrm{C}}}{16n \cdot \cos^4\alpha} - \frac{3}{16n \cdot \cos^2\alpha}\left[\sum_{m=1}^{2}\left(\frac{l_m^2 + h_m^2}{l_m}\theta_{\mathrm{C}} \cdot \delta T_{\mathrm{C}} - \frac{h_m h_{\mathrm{P}m}}{l_m}\theta_{\mathrm{P}} \cdot \delta T_{\mathrm{P}}\right) - (h_{\mathrm{P2}} - h_{\mathrm{P1}})\tan\alpha \cdot \theta_{\mathrm{P}} \cdot \delta T_{\mathrm{P}}\right] + \frac{h_{\mathrm{P1}} + h_{\mathrm{P2}}}{2}\theta_{\mathrm{P}} \cdot \delta T_{\mathrm{P}}$$

(2~~3~~5)

When $\alpha = 0$:

$$\delta D_0 = -\frac{3}{16n} l_0\theta_{\mathrm{C}} \cdot \delta T_{\mathrm{C}} - \frac{3}{16n}\sum_{m=1}^{2}\left(\frac{l_m^2 + h_m^2}{l_m}\theta_{\mathrm{C}} \cdot \delta T_{\mathrm{C}} - \frac{h_m h_{\mathrm{P}m}}{l_m}\theta_{\mathrm{P}} \cdot \delta T_{\mathrm{P}}\right) + \frac{h_{\mathrm{P1}} + h_{\mathrm{P2}}}{2}\theta_{\mathrm{P}} \cdot \delta T_{\mathrm{P}} \tag{2~~4~~6}$$

If $h_{\mathrm{P}m} = h_m$ and $\theta_{\mathrm{C}} \cdot \delta T_{\mathrm{C}} = \theta_{\mathrm{P}} \cdot \delta T_{\mathrm{P}}$ are adopted, Eqn. (~~24~~26) will become

$$\delta D_0 = -\frac{3}{16n} L\theta_C \cdot \delta T_C + \frac{h_{P1} + h_{P2}}{2} \theta_C \cdot \delta T_C = \left(-\frac{3}{16n} L + \frac{h_{P1} + h_{P2}}{2} \right) \theta_C \cdot \delta T_C \quad (275)$$

Since the suspender at the mid-span of the central span girder is short in length and thus undergoes little thermal deformation, the main cable and the girder have almost the same vertical displacement at the mid-span, as demonstrated by Ref. [6]. As a result, the thermally induced variation in the mid-span elevation of the central-span girder can take the value of δD_0 with use of Eqns. (253)–(275).

Moreover, the horizontal displacement of the tower top can be estimated by combining Eqns. (59) and (17):

$$\delta l_m = \frac{l_m^2 + h_m^2}{l_m} \theta_C \cdot \delta T_C - \frac{h_m \cdot h_{Pm}}{l_m} \theta_P \cdot \delta T_P \quad (2628)$$

If the tower top moves toward the central span, δl_m ($m = 1, 2$) will be positive. Assuming $h_{Pm} = h_m$ and $\theta_C \cdot \delta T_C = \theta_P \cdot \delta T_P$, Eqn. (2628) can be simplified as

$$\delta l_m = l_m \theta_C \cdot \delta T_C \quad (2729)$$

As $\delta l_0 = -(\delta l_1 + \delta l_2)$, the variation in the horizontal distance of the two tower tops is:

$$\delta l_0 = -\sum_{m=1}^{2} \left(\frac{l_m^2 + h_m^2}{l_m} \theta_C \cdot \delta T_C - \frac{h_m h_{Pm}}{l_m} \theta_P \cdot \delta T_P \right) \quad (2830)$$

Again in the simplified scenario,

$$\delta l_0 = -(l_1 + l_2) \theta_C \cdot \delta T_C \quad (2931)$$

The increase in the tower-top distance corresponds to a positive δl_0 in Eqns. (2830) and (2931).

Eqns. (2123), (2527), (2729), and (2931) are simplified formulas of displacement of different components. It is interesting that they show a unified form of the product of $\theta_C \cdot \delta T_C$ and a length, which can be defined as the temperature equivalent length, L_E. L_E takes different values for each responses. For example, $L_E = 3L/(16n)$ for δf_0 and $L_E = l_m$ for δl_m ($m = 1, 2$). As θ_C is a constant, the temperature-induced change in the above responses is dependent on L_E only.

The above derived temperature-induced deformation is summarized in Table 1.

Table 1 Summary of temperature-induced deformation calculation

Items	General formulas	Simplified formulas $L_E\theta_C \cdot \delta T_C$	Positive sign definition
Mid-span deflection change of the main-span cable (δf_0)	Eqn. (~~19~~21) (Eqn. (~~20~~22) for $\alpha = 0$)	$L_E = \frac{3}{16n}L$	The cable sag increases.
Mid-span elevation change of the main-span cable or girder (δD_0)	Eqn. (~~23~~25) (Eqn. (~~24~~26) for $\alpha = 0$)	$L_E = -\frac{3}{16n}L + \frac{h_{P1} + h_{P2}}{2}$	The mid-point goes upward.
Horizontal displacement of the tower top (δl_m; m = 1, 2)	Eqn. (~~26~~28)	$L_E = l_m$	The tower top moves toward the central span.
Horizontal distance change between tower tops (δl_0)	Eqn. (~~28~~30)	$L_E = -(l_1 + l_2)$	The distance increases.

* Note: $\alpha = 0$ is positive for the counter clockwise rotation from the horizontal.~~; l_m and h_{Pm} (m = 1, 2) take positive values.~~

3. Case Study of the Tsing Ma Bridge

The proposed formulas are applied to the Tsing Ma Bridge for verification. The field monitoring data on January 16–19, April 16–19, July 14–19, and October 26–29 in 2005 are used to investigate both the diurnal and seasonal variations in thermal deformations of the bridge.

3.1 Background of the bridge

The Tsing Ma Bridge is a vital link between the Hong Kong mainland and the Hong Kong International Airport. At its open to public in May 1997, it was the longest-span suspension bridge in the world carrying both highway and railway traffics. The stiffening girder is a steel truss structure. It has a total length of 2160 m, from the Ma Wan abutment to the Tsing Yi abutment (Figure 7~~Figure 6~~). Apart from the abutments at both ends, the girder is intermediately supported by the two 1377-m-apart towers, two piers in the Ma Wan side span (M1 and M2 in Figure 7~~Figure 6~~), and three piers in the Tsing Yi side span (T1–T3). The width and depth of the double-deck girder are respectively 41 m and 7.643 m, which allow it to accommodate dual three-lane expressway on the upper deck and two railway tracks plus two carriageways on the lower deck. Both concrete towers are 206.4 m high above the sea level,

Commented [XY6]: α is positive?

Field Code Changed

Field Code Changed

Field Code Changed

Field Code Changed

Commented [XY7]: ? when *l* and *h* are positive?

each with two legs connected by four portal beams.

The main cables have a diameter of approximately 1.1 m and are 36 m apart. The span arrangement of the main cables is 99.5+355.5+1377+300 m, with a horizontal distance between the two ground anchorages being 2132 m. The sag-to-span ratio of the main-span cables, n, is 1/10.8. The Ma Wan side-span cables are first held by saddles on pier M2 and then fixed on the gravity anchorage, while the Tsing Yi side-span cables are directly affixed to the anchorage. The suspenders are distributed evenly within the main span as well as the Ma Wan side span from pier M2 to the tower, with the distance between adjacent suspenders being 18 m.

The translational movements of the girder are restrained in three orthogonal directions (x-, y-, z-axes) at the Ma Wan abutment. Piers M1, T2, and T3 provide only the vertical translational restraint (z-axis) to the girder, while piers M2 and T1, both towers, and the Tsing Yi abutment provide both the lateral (y-axis) and vertical translational restraints. During the operational stage, the main cables are fixed at the tower tops and the anchor blocks, and on pier M2 there is also an intermediate support. Although the pier saddles on pier M2 slightly changes the geometric profile of the side span cable, it has negligible effect on the angle change of the cable.

A comprehensive SHM system on the Tsing Ma Bridge has been put into operation since 1997. The air and girder temperatures are measured by the PT100 Platinum resistance temperature sensors, and the cable temperature by the thermocouple sensors embedded inside the cable. No temperature sensors are installed on the towers. All temperature data are sampled at a rate of 0.07 Hz. The translational displacements of the key sections on the girder, cable, and tower are measured by the GPS rovers with a sampling frequency of 10 Hz. The elevation of the girder is also monitored by the level sensing stations, which convert the pressure change in the pipe system to the elevation difference. There are two pipe systems filled with water and oil, respectively, both sampled at 2.56 Hz. More details about the Tsing Ma Bridge and its SHMS can be found in Ref. [1].

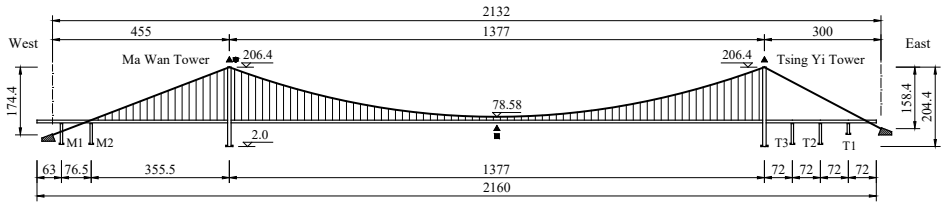

Figure 7 Elevation of Tsing Ma Bridge with sensors involved in this study (Unit: m; ▲: GPS rover, ■: level sensor, ●: thermocouple for cable temperature)

3.2 Field measurement data

Although the wind[22] and traffic[23] loadings could cause ~~obvious~~ structural displacements, the deformation of large-span suspension bridges during the normal in-service conditions is dominated by the temperature changes[1]. Since the ambient temperature changes in a slower rate than the dynamic loading such as winds and traffics, the time averaging can filter out the high frequency components in the raw data to a great extent while retaining the thermally induced structural responses[6]. In this regard, the hourly means of the measured temperature and displacement are analysed here.

The mid-span elevation variation of the main-span cable is measured by the GPS and level sensors. As demonstrated in Figure 8~~Figure 7~~(a), the GPS measurements have similar baselines to those by the oil-based level sensors (LSOs), while the data from the water-based level sensors (LSWs) have a downward offset. Figure 8~~Figure 7~~(b) illustrates the modified level-sensing data, and their baselines are adjusted according to the GPS data in each season. These three independent measuring systems captured the daily variation of δD_0 consistently, which provides a cross validation to the accuracy of the GPS system. The GPS data will thus be used hereafter for comparison with the analytical results.

Figure 9~~Figure 8~~ presents the time histories of the cable ~~effective~~ average temperature, the mid-span elevation of the main-span cable, and the horizontal displacement of the tower tops. ~~The cable effective temperature is the averages of the thermocouples across the cable section, and it~~During the year, the cable average ~~effective~~ temperature rose from 14 ºC in the winter to 38 ºC in the summer. As the temperature increased, the main-span cable moved downward and the yearly displacement was 1200 mm approximately. During the period, the two tower tops moved close to each other, with the

movements toward west being positive in the SHM system. In particular, the Ma Wan tower top experienced about 150 mm peak-to-peak horizontal displacement, while the Tsing Yi tower top moved about 90 mm.

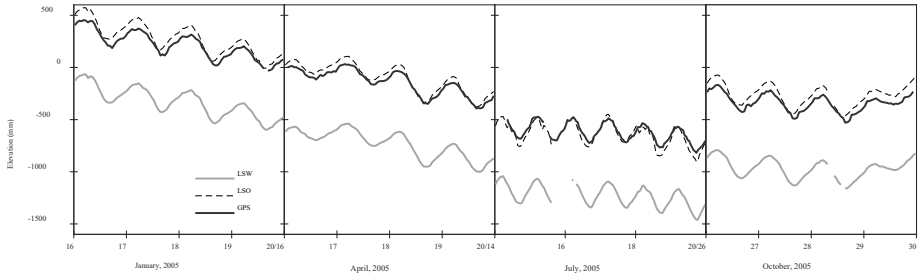

(a) Raw data

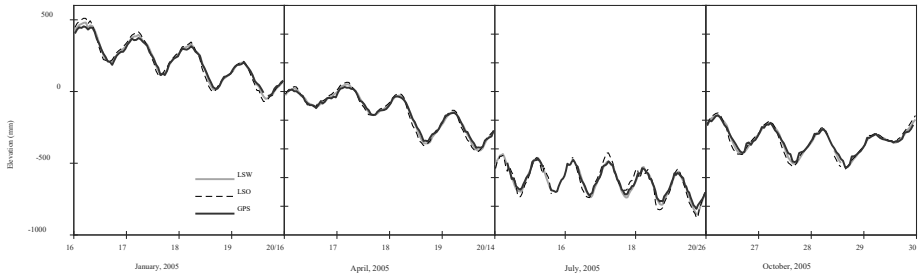

(b) Baselines of LSW and LSO are adjusted

Figure 8 Measured mid-span elevation of the main-span cable in 2005

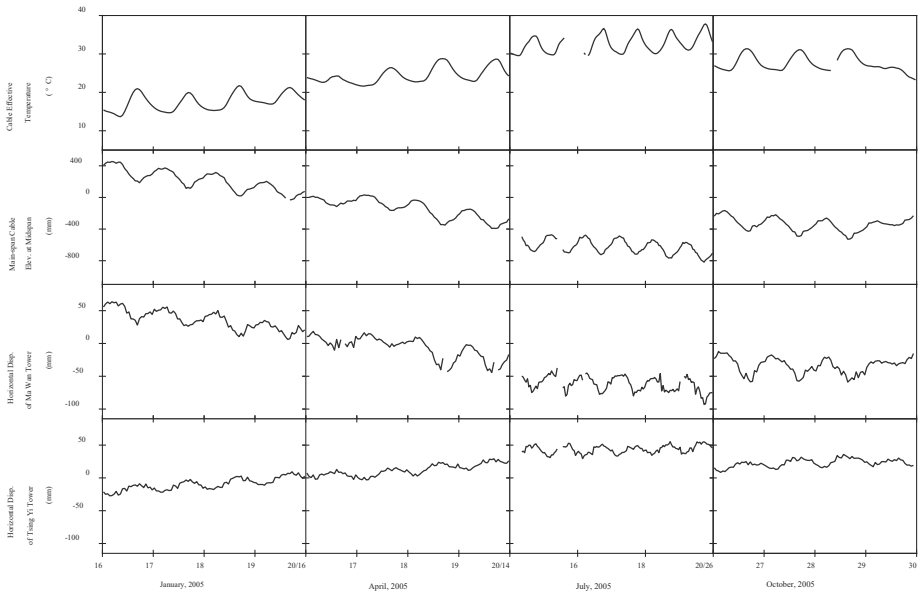

Figure 9 Cable effective temperature and bridge displacements in different seasons

3.3 Calculated displacement

In order to calculate the bridge responses to a given temperature change, the references or initial values of the temperature and structural responses are required. Here, the mean values of the 18-day measurements ~~measurements at 8.30 a.m. on 26th October 2005~~ are chosen as the reference values.~~, because the cable temperature at that time instant was almost in the middle of the temperature range.~~ The choice of the reference values will not affect the temperature sensitivity of the calculated structural responses as the formulas in Section 2 show.

As shown in Figure 7~~Figure 6~~, The main-, left side-, and right side-span cables have the span of $l_0 = 1377$ m, $l_1 = 455$ m, and $l_2 = 300$ m, respectively, with the horizontal distance of $L = 2132$ m between the two anchorages. The main-span cable has the sag $f_0 = 127.82$ m, leading to a sag-to-span ratio $n = 0.0928$. The two towers are of equal height $h_{P1} = h_{P2} = 204.4$ m with their tops at the same level, and thus the inclination $\alpha = 0$. The elevation difference between the supports of the side-span cable is respectively $h_1 = 174.4$ m and $h_2 = 158.4$ m. The linear expansion coefficients of the

steel of the cable and the concrete of the towers are $\theta_C = 1.2\times10^{-5}/°C$ and $\theta_P = 1.0\times10^{-5}/°C$, respectively.

The tower has no thermal sensors installed and the measured temperature is not available on the bridge. According to the FE simulation by Xia et al.[8], the variation range of the simulated temperature at the external surfaces of the bridge towers was close to that of the cable. Therefore, the measured temperature of the cables is used for the towers.

Given the temperature range, the mid-span elevation of the main-span cable is calculated from Eqns. (~~24~~26) and (2~~5~~7) and shown in Figure 10~~Figure 9~~. The calculated results have a good agreement with the measurement. As $\delta T_P = \delta T_C$ is adopted, both Eqns. (~~24~~26) and (27~~5~~) show the estimated elevation vary linearly with δT_C. Also, the difference between Eqns. (~~24~~26) and (~~25~~27) is negligible.

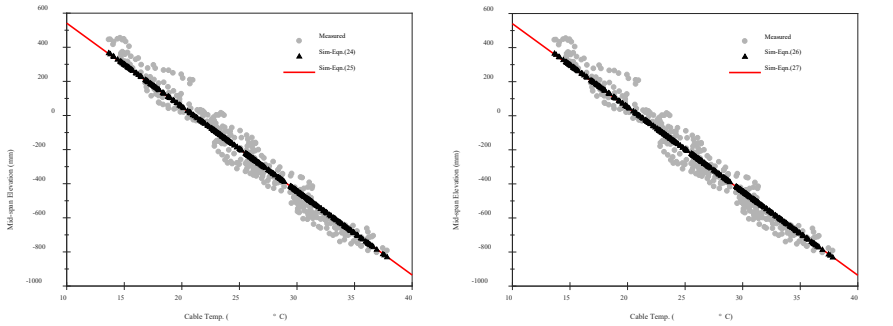

Figure 10 The measured and calculated mid-span elevation of the main-span cable

The horizontal displacement at the tower tops and the horizontal distance between them are calculated through Eqns. (~~26~~28)~~–~~(~~29~~31). The results are compared with the measurements in Figures 1~~0~~1 and ~~11~~12. In general, the calculated tower-top displacements versus the cable temperature match the measured ones well, and the simplified formulas Eqns. (~~27~~29) and (~~29~~31), which neglect the tower-related information through assumptions, produce almost similar values as Eqns. (~~26~~28) and (~~28~~30).

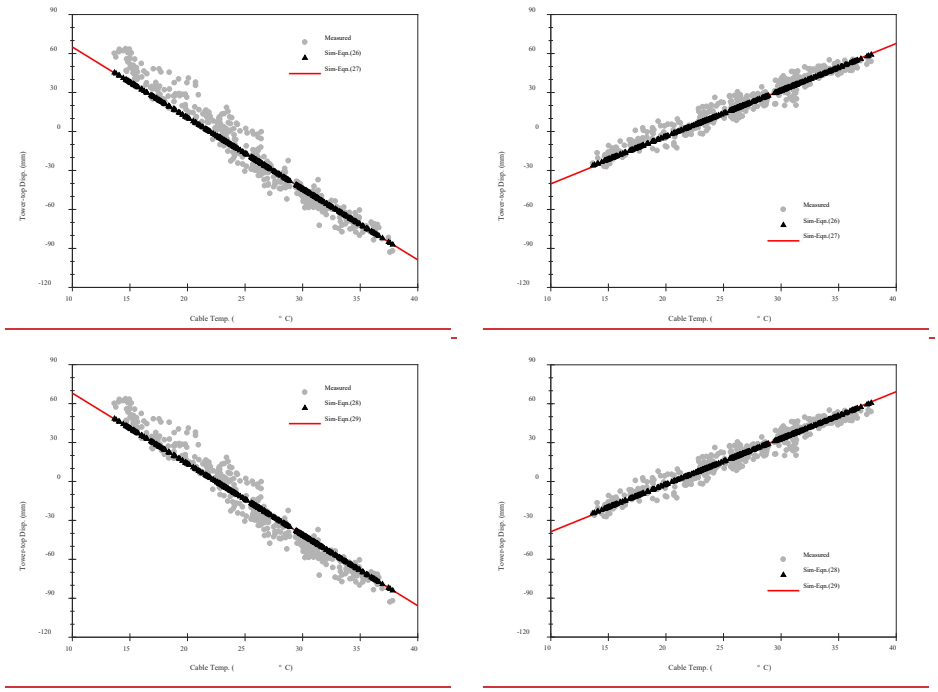

(a) Ma Wan tower (b) Tsing Yi tower

Figure 11 The measured and calculated tower-top longitudinal horizontal displacement

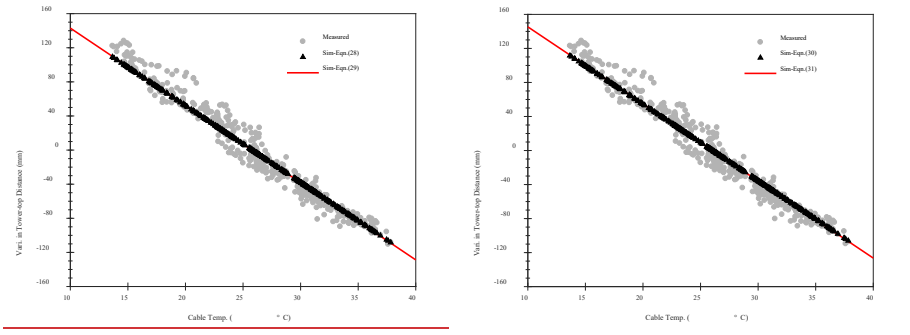

Figure 12 The measured and calculated variation in tower-top distance

3.4 Comparison

Section 3.3 has proven the effectiveness of the formulas in Section 2, which provide us with valuable

insights into the thermal deformation of suspension bridges.

(1) Displacements of different bridge components

The thermal responses in this study are approximated by the linear superposition of the cable and tower temperature effects. In the simplified cases ($\theta_C \cdot \delta T_C = \theta_P \cdot \delta T_P$, $h_{Pm} = h_m$, and $\alpha = 0$), all bridge displacements studied here are proportional to $\theta_C \cdot \delta T_C$. In particular,

1) δf_0 is proportional to L and $1/n$, and δD_0 has an additional item proportional to the average height of the towers.

2) δl_m ($m = 1, 2$) and δl_0 are proportional to the span of side-span cables.

The ratio of the magnitudes of δf_0, δD_0, δl_m ($m = 1, 2$), and δl_0 is:

$$|\delta f_0| : |\delta D_0| : |\delta l_0| : |\delta l_m| = \frac{3(l_0 + l_1 + l_2)}{16n} : \left[\frac{3(l_0 + l_1 + l_2)}{16n} - \frac{h_{P1} + h_{P2}}{2}\right] : (l_1 + l_2) : l_m \tag{30}$$

As $n \approx 1/10$, $3/(16n) \approx 2$, δf_0 and δD_0 are larger than δl_m and δl_0. For the Tsing Ma Bridge, $|\delta f_0| : |\delta D_0| : |\delta l_0| : |\delta l_1| : |\delta l_2| = 1 : 0.95 : 0.18 : 0.11 : 0.07$. The mid-span vertical displacements of the main-span cable or girder are approximately 10 times the tower-top horizontal displacement.

(2) Contribution of different factors to the bridge displacement

The contributions of the temperature variation in the main-span cable (Factor 1), side-span cable (Factor 2), and the tower (Factor 3) are compared in Table 2, in which the Tsing Ma Bridge ($\alpha = 0$) is used as an example. For comparison, the sensitivity of the structural responses with respect to the cable temperature, i.e., the displacement per unit temperature change, is calculated with the assumption of $\delta T_P = \delta T_C$.

For the mid-span deflection change of the mid-span cable (Item 1 in Table 2), three factors contribute 65%, 43%, and −7%. In the general case, the relative contribution of the three factors to δf_0, referring to Eqn. (~~19~~21), is

$$Factor1 : Factor2 : Factor3 = \left(\frac{l_0 \theta_C \cdot \delta T_C}{\cos^2 \alpha}\right) : \left(\sum_{m=1}^{2} \frac{l_m^2 + h_m^2}{l_m} \theta_C \cdot \delta T_C\right) : \left(-\sum_{m=1}^{2} \frac{h_m h_{Pm}}{l_m} \theta_P \cdot \delta T_P - \tan\alpha (h_{P2} - h_{P1}) \theta_P \cdot \delta T_P\right)$$

Field Code Changed

(31)

Because the spans of a suspension bridge (l_m; $m=0,1,2$) are generally larger than the height (h_m and h_{Pm}; $m=1,2$), Factors 1 and 2 (representing the cable temperature) contribute more than Factor 3 (the tower temperature). The similar conclusion applies to δD_0 (Item 2 in Table 2).

For the tower-top horizontal displacement, Factors 2 and 3 play opposite roles with a negligible influence of Factor 1. According to Eqn. (~~26~~28), their contribution ratio is

$$Factor2 : Factor3 = \left[\left(l_m^2 + h_m^2\right)\theta_C \cdot \delta T_C\right] : \left(-h_m h_{Pm} \theta_P \cdot \delta T_P\right) \tag{32}$$

For most towers, Factor 2 has a larger contribution than Factor 3, which means the cable temperature is also the dominant factor of the tower-top movement. For the Tsing Ma Bridge, Factor 3 contributes about one-sixth of Factor 2 to the tower-top horizontal movements, as shown in Table 2. Since Factor 1 drops out from the calculation of the tower-top horizontal displacements, the tower temperature has a relatively larger contribution to l_m ($m=0,1,2$, about 15–30%) than to δf_0 and δD_0 (about 10%).

Table 2 Contribution of three factors to thermal deformation of the Tsing Ma Bridge

Items	Factor 1	Factor 2	Factor 3	Total	Formula
(1) Mid-span deflection change of the main-span cable, δf_0 (mm/°C)	33.38 (65%)	21.95 (43%)	−3.76 (−7%)	51.56 (100%)	Eqn. (220)
(2) Mid-span elevation change of the main-span cable, δD_0 (mm/°C)	−33.38 (67%)	−21.95 (44%)	5.81 (−12%)	−49.52 (100%)	Eqn. (~~24~~26)
(3) Horizontal displacement of the Ma Wan tower top, δl_1 (mm/°C)	0 (0)	6.26 (114%)	−0.78 (−14%)	5.48 (100%)	Eqn. (~~26~~28)
(4) Horizontal displacement of the Tsing Yi tower top, δl_2 (mm/°C)	0 (0)	4.60 (131%)	−1.08 (−31%)	3.52 (100%)	Eqn. (~~26~~28)
(5) Variation in tower-top horizontal distance, δl_0 (mm/°C)	0 (0)	−10.87 (121%)	1.86 (−21%)	−9.00 (100%)	Eqn. (~~28~~30)

Note: The values in brackets are the percentage of the total displacement.

3.5 Discussions

From Figures 10~~9~~–12~~1~~ the calculated thermal responses agree well with the mean of the measurement for a given temperature. The dispersion around the calculated means still exists in the measurement data, which might come from the following reasons in addition to the measurement errors: (1) the bridge displacements caused by other loadings as traffics and winds are included in the measurement data; (2) the tower temperature is not equal to the cable temperature from time to time; (3) the assumptions adopted in the analytical derivation are over-simplified.~~,~~ For example,~~e.g.,~~ the sag effect of the side-span cables (especially for those suspending a deck) is not considered, and the flexural~~e~~ stiffness ~~properties~~ and internal force changes of structural components are also neglected.

Commented [XY8]: Again, is this flexural deformation?

Although the tower temperature does not dominate the global thermal deformation of suspension bridges, it still accounts for about 10% and 20% of the variation in mid-span elevation and tower-top displacement. To better predict the thermal deformation with high accuracy, temperature sensors should be designed and installed on towers in SHM systems.

4. Conclusions

This study reveals the physical mechanisms of temperature-induced deformations of the girder, main cables, and towers of long-span suspension bridges. General models and analytical formulas are developed, which offer a quantitative approach to estimate the thermal deformation and explain the observed phenomena in the Tsing Ma Bridge intuitively. The main conclusions are drawn as follows:

(1) The mid-span elevation of the main-span cable and girder decreases as the temperature increases, which is a combined effects of three factors: the main-span cable, the side-span cable, and the tower temperatures. The cable temperature (both main- and side-span) contributes most.

(2) The tower-top longitudinal displacement of ground anchored suspension bridges is a combined effect of the side-span cable and the tower temperature. These two mechanisms have opposite effects on the tower-top movement, and the former is the dominant factor. When the side-span cable temperature increases, both towers deflect toward the middle span and the longitudinal

horizontal distance between tower tops decreases. The temperature change of the mid-span cable has negligible effect on the tower movement.

(3) Assuming the changes of the tower and cable temperatures of a ground anchored suspension bridge are equal, a unified formula of the temperature-induced bridge deformation is derived, which is the product of the temperature effective length L_E, linear expansion coefficient of the cable θ_C, and the cable temperature change δT_C. L_E varies for different responses.

The proposed general formulas are based on physical models. They have merits of clear concepts, simple calculation, and general applicability, which make them suitable for the quick calculation or approximation of the deformation of suspension bridges under temperature change. This study provides valuable physical interpretation and prior knowledge on the thermal deformation of suspension bridges, which could help to improve structural preliminary design, guide monitoring schemes, and optimize load–response baseline models. ~~Future work will investigate~~ The sag effect of the side-span cables, the lateral movement ~~in the direction perpendicular to the bridge axis~~of the cables and towers, and the temperature effects of the self-anchored and multiple-tower suspension bridges will be investigated in future.

Acknowledgments

The authors express their appreciation for the financial support provided by the Hong Kong Scholars Program (Grant no.: XJ2018062), the National Natural Science Foundation of China (Grant no.: 51608034), and the Fundamental Research Funds for the Central Universities (Grant no.: FRF-TP-18-028A2). We are thankful for the significant assistance received from the Highway Department of the Government of Hong Kong Special Administrative Region.

Conflicts of Interest

The authors declare no conflicts of interest.

References

[1] Xu Y L, Xia Y. Structural Health Monitoring of Long-Span Suspension Bridges. Abingdon: Spon Press, 2011.

[2] Yarnold M T, Moon F L. Temperature-based Structural Health Monitoring Baseline for Long-Span Bridges.

Engineering Structures. 2015, 86: 157-167.

[3] Zhou G, Yi T, Chen B, et al. Modeling Deformation Induced by Thermal Loading Using Long-Term Bridge Monitoring Data. Journal of Performance of Constructed Facilities. 2018, 32(3): 04018011.

[4] Cao Y, Yim J, Zhao Y, et al. Temperature Effects on Cable Stayed Bridge Using Health Monitoring System: A Case Study. Structural Health Monitoring. 2011, 10(5): 523-537.

[5] Zhou Y, Sun L. A Comprehensive Study of the Thermal Response of a Long-Span Cable-Stayed Bridge: From Monitoring Phenomena to Underlying Mechanisms. Mechanical Systems and Signal Processing. 2019, 124: 330-348.

[6] Xu Y L, Chen B, Ng C L, et al. Monitoring Temperature Effect on a Long Suspension Bridge. Structural Control and Health Monitoring. 2010, 17(6): 632-653.

[7] Brownjohn J M W, Koo K, Scullion A, et al. Operational Deformations in Long-Span Bridges. Structure and Infrastructure Engineering. 2015, 11(4): 556-574.

[8] Xia Y, Chen B, Zhou X, et al. Field Monitoring and Numerical Analysis of Tsing Ma Suspension Bridge Temperature Behavior. Structural Control and Health Monitoring. 2013, 20(4): 560-575.

[9] Koo K Y, Brownjohn J M W, List D I, et al. Structural Health Monitoring of the Tamar Suspension Bridge. Structural Control and Health Monitoring. 2013, 20(4): 609-625.

[10] Westgate R, Koo K, Brownjohn J M W. Effect of Solar Radiation on Suspension Bridge Performance. Journal of Bridge Engineering. 2015, 20(5): 04014077.

[11] Kashima S, Yanaka Y, Suzuki S, et al. Monitoring the Akashi Kaikyo Bridge: First Experiences. Structural Engineering International. 2001, 11(2): 120-123.

[12] Guo T~~ong~~, Li A~~iqun~~, Li J~~ianhui~~. Fatigue Life Prediction of Welded Joints in Orthotropic Steel Decks Considering Temperature Effect and Increasing Traffic Flow. Structural Health Monitoring. 2008, 7(3): 189-202.

[13] Xia Q, Zhang J, Tian Y, et al. Experimental Study of Thermal Effects on a Long-span Suspension Bridge. Journal of Bridge Engineering. 2017, 22(7): 4017034.

[14] Li X, Ren W, Zhong J. Making Good Use of Suspension Bridge Health Monitoring System. *In* Proceedings of the 1st International Conference on Civil Engineering, Architecture and Building Materials (CEABM 2011). Haikou, China, 2011: 250-253.

[15] Kim S, Kim C, Lee J. Monitoring Results of a Self-Anchored Suspension Bridge. *In* Sensing Issues in Civil Structural Health Monitoring, Ansari F. Dordrecht, Netherlands: Springer, 2005: 475-484.

[16] Zhou G, Li A, Li J, et al. Health Monitoring and Comparative Analysis of Time-dependent Effect Using Different Prediction Models for Self-anchored Suspension Bridge with Extra-wide Concrete Girder. Journal of Central South University. 2018, 25(9): 2025-2039.

[17] Wollmann G P. Preliminary Analysis of Suspension Bridges. Journal of Bridge Engineering. 2001, 6(4): 227-233.

[18] Timoshenko, S P, Young, H D. Theory of Structures. 2nd ed. New York, United States: McGraw-Hill, Inc., 1965.

[19] Zhou Y, Sun L. Insights into Temperature Effects on Structural Deformation of a Cable-Stayed Bridge Based on Structural Health Monitoring. Structural Health Monitoring. 2019, 18(3): 778-791.

[20] Ministry of Transport of the People's Republic of China. Specifications for Design of Highway Suspension Bridge. Beijing, China: China Communications Press, 2015.

[21] Su J, Xia Y, Ni Y, et al. Field Monitoring and Numerical Simulation of the Thermal Actions of a Supertall Structure. Structural Control and Health Monitoring. 2017, 24(4): e1900.

[22] Mao J X, Wang H, Feng D M, et al. Investigation of Dynamic Properties of Long-span Cable-stayed Bridges Based on One-year Monitoring Data under Normal Operating Condition. Structural Control and Health Monitoring. 2018, 25(5): e2146.

[23] Mao J X, Wang H, Li J, et al. Fatigue Reliability Assessment of a Long-span Cable-stayed Bridge Based on One-year Monitoring Strain Data. Journal of Bridge Engineering. 2019, 24(1): 05018015.

Appendix A

This part serves to derive the length of a single-span sagged cable (Figure A1) subjected to a uniformly distributed vertical load along its span, which is analogue to the cable bearing the weight of the suspended girder in a suspension bridge.

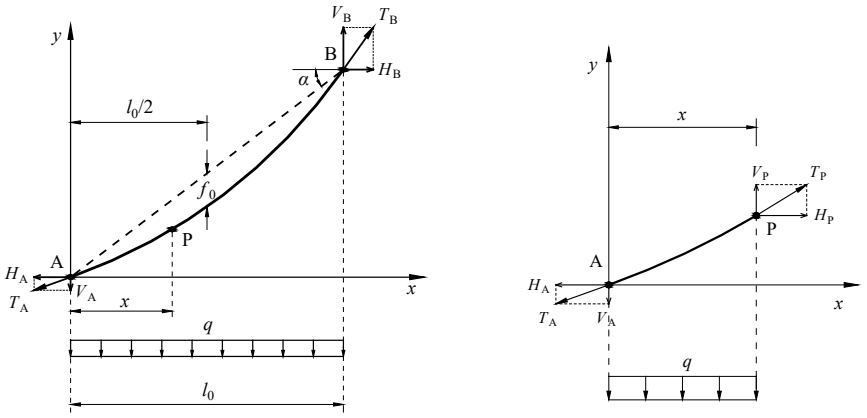

(a) A single-span sagged cable (b) Free body diagram of the AP segment

Figure A1 Analytical model of a sagged cable under uniformly distributed vertical load

The suspended cable APB in the figure has a span of l_0 and a uniformly distributed vertical load q. The lower end A is set as the origin of the Cartesian coordinate *xoy*. The chord AB of this cable has an inclination angle α to the horizontal line. Point P is an arbitrary point on the cable. Assume the cable has no bending stiffness. The tension force and its horizontal and vertical components at Point i ($i = \mathrm{A, B, P}$) are respectively denoted as T_i, H_i, and V_i. According to the equilibrium of the horizontal force for the cable APB and AP segment (Figure A1(b)), we have:

$$H_{\mathrm{A}} = H_{\mathrm{P}} = H_{\mathrm{B}} = H_0 \tag{A1}$$

Hence, the horizontal component of the tension in the cable is a constant, denoted as H_0.

The equilibrium of moment about the upper support B for the cable APB gives the vertical reaction at point A:

$$V_{\mathrm{A}} = H_0 \tan\alpha - \frac{ql_0}{2} \tag{A2}$$

The vertical component of the tension at Point P can be expressed as

$$V_{\mathrm{P}} = H_0 \frac{dy}{dx} \tag{A3}$$

The equilibrium of vertical force for the AP segment leads to:

$$V_{\mathrm{P}} - qx - V_{\mathrm{A}} = 0 \tag{A4}$$

Substitute Eqns. (A2) and (A3) into Eqn. (A4):

$$H_0 \frac{dy}{dx} = H_0 \tan\alpha - \frac{ql_0}{2} + qx \tag{A5}$$

The equation of the cable curve in terms of position x can be obtained through integration of Eqn. (A5)

$$y = \left(\tan\alpha - \frac{ql_0}{2H_0} \right) x + \frac{q}{2H_0} x^2 + c_1 \tag{A6}$$

The integration constant c_1 can be determined from the boundary condition at point A, i.e. $y = 0$ at $x = 0$, yielding $c_1 = 0$. The cable shape is a parabola:

$$y = x \tan\alpha + \frac{q}{2H_0} \left(x^2 - l_0 x \right) \tag{A7}$$

The deflection f at any point on the cable is equal to the vertical distance between the parabola and the chord AB, that is

$$f = x \tan\alpha - y = \frac{q}{2H_0} \left(l_0 x - x^2 \right) \tag{A8}$$

The maximum deflection occurs at the mid-span, $x = l_0/2$, at which

$$f_0 = \frac{ql_0^2}{8H_0} \tag{A9}$$

The sag-to-span ratio n is

$$n = \frac{f_0}{l_0} = \frac{ql_0}{8H_0} \tag{A10}$$

Substituting Eqn. (A10) into Eqn. (A7), we have another form of the cable curve expression:

$$y = x\tan\alpha + \frac{4n}{l_0}\left(x^2 - l_0 x\right) \tag{A11}$$

The total length of the cable, S_0, can be calculated through integration:

$$S_0 = \int_0^{l_0}\sqrt{1+\left(\frac{dy}{dx}\right)^2}\,dx = \int_0^{l_0}\sqrt{1+\left[\tan\alpha + \frac{4n}{l_0}\left(2x - l_0\right)\right]^2}\,dx \tag{A12}$$

Using the substitution method, i.e. $u = 4n\left(2x - l_0\right)/l_0$, Eqn. (A12) becomes

$$S_0 = \int_{-4n}^{4n}\frac{l_0}{8n}\sqrt{1+\left(\tan\alpha + u\right)^2}\,du \tag{A13}$$

The integral function $g\left(u\right) = \sqrt{1+\left(\tan\alpha + u\right)^2}$ in Eqn. (A13) is approximated with the first six terms in the Maclaurin series, and then the result can be calculated as

$$S_0 \approx \int_{-4n}^{4n}\frac{l_0}{8n}\left(\sum_{m=0}^{5}\frac{g^{(m)}(0)}{m!}u^m\right)du = l_0\left[\sec\alpha + \frac{8}{3}n^2\cos^3\alpha - \frac{32}{5}n^4\left(5\cos^7\alpha - 4\cos^5\alpha\right)\right] \tag{A14}$$

This is the approximate expression of the cable length S_0 used in Section 2.

Appendix B

This part presents the finite element analysis (FEA) results of the Tsing Ma Bridge to justify the assumptions adopted in Section 2. The FE model of the bridge (Figure B1) comprises 23,960 nodes and 28,856 elements. The main cables and the suspenders are modelled using bar elements, the towers using solid elements, the girder and the piers using three-dimensional beam elements, and the deck plate of the girder using solid elements. This model is calibrated using the measured dynamic properties of the bridge. More details can be found in Ref. [8].

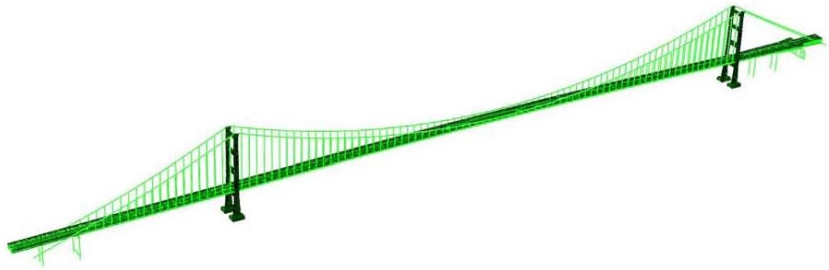

Figure B1 Finite element model of the Tsing Ma Bridge

A unit temperature increase is applied to the main- and side-span cables and the two towers of the bridge model separately. The changes in the mid-span elevation of the main-span cable as well as the horizontal and vertical displacements of both tower tops are calculated. The temperature sensitivities of structural displacements with respect to each temperature variable are listed in Table B1, as compared with the proposed analytical results.

Table B1 Temperature sensitivities calculated by the proposed formulas and the FE model (Unit: mm/ºC)

Items*		A unit temperature increase in bridge components				
		Main-span Cable ($j=1$)	Ma Wan Side-span Cable ($j=2$)	Tsing Yi Side-span Cable ($j=3$)	Ma Wan Tower ($j=4$)	Tsing Yi Tower ($j=5$)
Mid-span elevation of main-span cable ($i=1$)	Formula	−33.4	−12.6	−9.3	2.6	3.2
	FEA	−32.9	−10.5	−8.0	2.7	3.0

Horizontal disp. of Ma Wan tower top ($i=2$)	Formula	0	6.3	0	−0.8	0
	FEA	−0.4	5.3	−0.1	−0.8	0
Horizontal disp. of Tsing Yi tower top ($i=3$)	Formula	0	0	4.6	0	−1.1
	FEA	−0.4	−0.1	4.1	0	−1.0
Vertical disp. of Ma Wan tower top ($i=4$)	Formula	0	0	0	2.0	0
	FEA	0	0	0	2.0	0
Vertical disp. of Tsing Yi tower top ($i=5$)	Formula	0	0	0	0	2.0
	FEA	0	0	0	0	2.0

* Positive sign definition: For vertical displacements the point goes upward, whereas for horizontal displacements the point moves toward the central span.

The temperature sensitivities are denoted as S_{ij}^{k}, where the subscript $i=1,2,\cdots,5$ represents five responses, $j=1,2,\cdots,5$ stands for temperature in five bridge components, and the superscript $k=\mathrm{A}$ or F is for analytical and FEA results, respectively.

(1) Assumption in Section 2.1

When the temperature of the main-span cable changes, the tower-top horizontal displacement (S_{21}^{F} or S_{31}^{F}) is only −0.4 mm/ºC. S_{41}^{F} and S_{51}^{F} are close to zero. Therefore, the assumption in Section 2.1 that both end supports of the main-span cable do not move horizontally and vertically is reasonable.

(2) Assumption in Section 2.2

When the temperature of the Ma Wan side-span cable increases, the FEA calculated horizontal displacement of the Ma Wan tower top is 5.3 mm/ºC, which is close to the analytical one (6.3 mm/ºC). So does the case for the Tsing Yi side-span cable and tower, i.e., 4.1 mm/ºC versus 4.6 mm/ºC. This justifies the ignorance of the cable tension changes in Section 2.2.

(3) Assumption~~s~~ in Section 2.3

When the temperature of the Ma Wan or Tsing Yi tower increases, the FEA calculated tower-top~~mid-span~~ horizontal displacement~~elevation change of the main span cable~~ (S_{24}^{F} and S_{35}^{F}) is close

to the analytical counterparts (S_{24}^{A} and S_{35}^{A}), and the tower-top elevation changes S_{44}^{F} and S_{44}^{A} (also S_{55}^{F} and S_{55}^{A}) have negligible difference. ~~-~~ This indicates that ~~the sag change induced by the inclination change of the main span cable chord due to the tower height change can be neglected. Moreover, the negligible difference between S_{44}^{F} and S_{44}^{A} (also S_{55}^{F} and S_{55}^{A}) indicates that~~ the cable tension changes due to the tower ~~top~~ height~~elevation~~ change have little influence on the movement~~vertical displacement~~ of the tower top, as assumed in Section 2.3.